Analysis of Time–Varying Mesh Stiffness for the Planetary Gear System with Analytical and Finite Element Methods

Ali Shahabi
Department of Mechanical Engineering,
University of Sistan and Baluchestan, Zahedan, Iran
Nedayedanesh Institute of Higher Education of Hormozgan,
Bandar Abbas, Iran
E-mail: alishahabi@pgs.usb.ac.ir

Amir Hossein Kazemian*
Department of Mechanical Engineering,
University of Sistan and Baluchestan, Zahedan, Iran
E-mail: kazemian@eng.usb.ac.ir
*Corresponding author

Received: 8 August 2020, Revised: 27 November 2020, Accepted: 1 December 2020

Abstract: In dynamic model of planetary gears, one of the key design parameters and one of the main sources of vibration is time–varying mesh stiffness of meshing gears. According to previous researches, the finite element method and analytical method are two techniques to estimate the mesh stiffness of meshing gears. In this work, in an innovation the periodically time–varying mesh stiffness of meshing gears is examined by both of finite element and analytical methods. The planetary gear set is modeled as a set of lumped masses and springs. Each element such as sun gear, carrier, ring gear and planets possesses three degrees of freedom and is considered as rigid body. The influence of effective parameters on the mesh stiffness of meshing gears and also numerical results of natural frequencies and vibration modes of the system are obtained. Based on the results, the influence of the higher pressure angles on the mesh stiffness of meshing gears is perceptible. By using the proposed mesh stiffness of meshing gears, for the system with numbers of odd and even equally and unequally spaced planets, natural frequencies and vibration modes are validated with a high accuracy.

Keywords: Pressure angle, Meshing gears, Vibration mode, Natural frequency.

How to cite this paper Ali Shahabi and Amir Hossein Kazemian, "Analysis of Time–Varying Mesh Stiffness for the Planetary Gear System with Analytical and Finite Element Methods", Int J of Advanced Design and Manufacturing Technology, Vol. 15/No. 1, 2022, pp. 157–166.
DOI: 10.30495/admt.2021.1906469.1210.

Biographical notes: Ali Shahabi is a PhD student in Mechanical Engineering at University of Sistan and Baluchestan, Zahedan, Iran. His current research interest includes dynamic and vibration of gear systems (planetary gear sets), control of suspension systems and vehicle's stability. He received his MSc in Mechanical Engineering from Shahid Bahonar University of Kerman, Iran, in 2014. **Amir Hossein Kazemian** received his PhD in Mechanical Engineering from Shahid Bahonar University of Kerman in 2017. He is currently Assistant Professor of Mechanical engineering at University of Sistan and Baluchestan, Zahedan, Iran. His current research focuses on dynamic, vibration and control of suspension and vehicle systems.

1 INTRODUCTION

In industry applications, planetary gears are generally used in power transmission systems. Dynamic loads, noise and reduction of the structural life are resulted from the planetary gear vibrations. Because of complexity and difficulty in the dynamic model, analysis of the dynamic for planetary gear sets is harder and complex than the other gear systems such as spur gears. In the dynamic model of planetary gears, key design factors are: mesh stiffness, bearing (support) stiffness, moments of inertia and component masses. Planetary gears are widely used in the aerospace, aircraft, wind turbine, marine and automotive applications and mining equipment. Some advantages and some positive points of planetary gear systems are: compactness, high torque to weight ratio and low noise, small radial bearing loads due to axi–symmetric orientation, high speed reduction in small volumes and also co–axial shaft arrangements.

The main source of vibration in planetary gear systems is the periodically time–varying mesh stiffness of sun–planet and ring–planet.

A nonlinear time–varying dynamic model for a planetary gear system with time–varying mesh stiffness and other nonlinearities was investigated in [1, 2]. Lin and Parker [3] modelled the time-varying mesh stiffness of the sun–planet and ring–planet meshes as rectangular waveforms with different contact ratios and mesh phasing. Sun and Ha [4] established a lateral–torsional coupled model with multiple backlashes, time-varying mesh stiffness, error excitation and sun-gear shaft compliance. A computer simulation based approach to study the effect of shaft misalignment and friction on total effective mesh stiffness for spur gear pair was proposed by Saxena et al. [5]. A finite element model of the geared rotor system established by Hao et al. [6] with the linear mesh stiffness of engaged helical gears. Parker and Lin [7] showed that the multiple tooth meshes in planetary gears have varying numbers of teeth in contact under operating speed.

Inalpolat and Kahraman [8] proposed a nonlinear time–varying dynamic model to predict modulation sidebands of planetary gear sets with periodically time–varying mesh stiffness. Wei et al. [9] improved the interval harmonic balance method (IHBM) to solve the dynamic problems of gear systems with backlash nonlinearity and time-varying mesh stiffness under uncertainties. Ambarisha and Parker examined nonlinear dynamic behaviour of spur planetary gears using two models [10]: lumped–parameter model and finite element model. Li et al. [11] established a batch module called “integration of finite element analysis and optimum design” by taking gear systems as testing examples. Meanwhile, dynamic of a lumped–parameter gear model by considering the effects of time–varying nonlinearity was formulated by Chen et al. [12] to investigate the spur gear rattle response under the idling condition. Kahraman [13, 14] developed a nonlinear time-varying dynamic model of a planetary transmission with an arbitrary number of pinions and proposed purely torsional model of the planetary gear system.

Liu et al. [15] considered time–varying stiffness and internal and external excitations to analysis gear system under fractional–order PID control with the feedback of meshing error change rate. Masoumi et al. [16] studied the dynamic scenario of planetary gears with a lumped mass two–dimensional model under time–varying stiffness of gears. Sainsot et al. [17] presented an improved fillet/foundation compliance analysis based on the theory of Muskhelishvili applied to circular elastic rings and they derived an analytical formula for gear body–induced tooth deflections. Shen et al. [18] established the dynamical model of a spur gear pair with time–varying stiffness and static transmission error under uncertainties and they extended the Incremental Harmonic Balance Method (IHBM) to study the nonlinear dynamics of a spur gear pair. In order to study on a dynamic model of the gear pair with multi-state mesh and time-varying parameters, Shi et al [19] considered effects of teeth separation and back–side tooth mesh. Wang and Howard [20] proposed the results of a detailed analysis of torsional stiffness of a pair of involute spur gears in mesh using finite element methods.

Zhou et al. [21] developed a modified mathematical model for simulating gear crack from root with linear growth path in a pinion by using an improved potential energy method to calculate the time-varying meshing stiffness of the meshing gear pair. The mesh stiffness of a gear under tooth faults such as tooth chip, tooth crack, and tooth breakage was derived by Tian et al. [22]. Jin et al. [23] developed a bending– torsional coupled dynamic model of the system by considering the lumped parameter method, and the influence of stiffness, damping and backlash and they solved numerically the dynamic equations. The complicated phenomenon of contact tooth pairs alternation between one and two during meshing was considered by Yang and Sun [24]. Lin and Parker [25] studied the free vibration of single–stage planetary gear sets and they examined natural frequencies and classified vibration modes into three types of translational, rotational and planet modes.

In this research, the dynamic and mesh stiffness of meshing gears in the single–stage spur planetary gear are investigated. According to previous researches, the mesh stiffness of meshing gears is evaluated by finite element [10, 20] and analytical methods [17, 24]. In this study, the mesh stiffness is investigated by both of finite element and analytical methods and unlike previous researches [25], the main source of vibration; i.e., the periodically time–varying mesh stiffness of meshing gears is examined. The single mesh stiffness of a tooth pair for spur gears (gear and pinion) is investigated by analytical calculation. In an innovation, the mesh stiffness of a tooth pair is expanded to the mesh stiffness of sun–planets and ring–planets in the planetary gear system as the function of first planet rotation. The periodically time–varying mesh stiffness of sun–planets and ring–planets is examined in the form of Fourier series and the finite element method by the polynomial estimation function. Furthermore, the influence of pressure angles on the mesh stiffness is investigated. Finally, for geometrical structures of the system (equally and unequally spaced planets) numerical results of natural frequencies and vibration modes are examined.

2 DYNAMIC MODEL OF THE PLANETARY GEAR

Two–dimensional (2D) lumped–parameter model of the single–stage spur planetary gear system is shown in "Fig. 1". Each element such as carrier (c), ring (r), sun (s) and J planets is assumed to have rigid behavior, i.e., lumped parameter system. The sun gear and carrier are connected to the input and output shaft, respectively. The external torque and force are applied to the input shaft (τ_s and F_s) and the ring gear is held stationary. Planet bearings are connected to the carrier and they are free to rotate and also translate with respect to it. The mass and moment of inertia of bearings are: m_i and I_i for $i = c, r, s, j$ and $j = p1, p2, \dots, J$ where J is number of planets and p denotes to the planet. Bearings are modeled by springs in x and y directions which are represented translational stiffness of bearings ($K_{ix}, K_{iy}, i = c, r, s$). The rotational stiffness of bearings ($K_{i\theta}, i = c, r, s$) is modeled by spring in the rotational direction of θ and stiffness of the planet bearing is represented by K_j. The translational and rotational coordinates of the carrier, ring and sun are: x_i, y_i and θ_i where $i = c, r, s$. The radial and tangential coordinates are: ξ_j and η_j which are known as translational coordinates of the planets center. The rotational coordinate of planets is: $u_j = r_j\theta_j$ and θ_j shows the rotation of planets.

In the present model, each element has three degrees of freedom in planar motion: two translations and one rotation and the system has $3(J + 3)$ degrees of freedom. The base radius for bearings of the ring, sun, carrier and planets is shown by $r_i, i = c, r, s, j$. For the carrier bearing r is the circle radius passing through the centers of planets.

In the present model ("Fig. 2"), the stiffness and rigidity of gear teeth and gear bodies are simulated by springs.

In "Fig. 2", the mesh of sun– jth planet and ring– jth planet is shown. As an example for the mesh of sun– jth planet, the circumferential jth planet location is identified by time–varying angle of $\psi_j(t)$ and the stiffness between sun and jth planet ($k_{sj}(t)$) acting along the action line. The static transmission error ($e_{sj}(t)$) is included as dynamic excitation at one end of the mesh spring and the pressure angle between sun and jth planet is $\alpha_{sj}(t)$. In "Fig. 1", coordinates of this study are shown and $\psi_j(t)$ are depended on the unit vector's rotation (**i** unit vector). $\psi_j(t)$ can be measured counter–clockwise from the first planet, so that $\psi_{p1} = 0$.

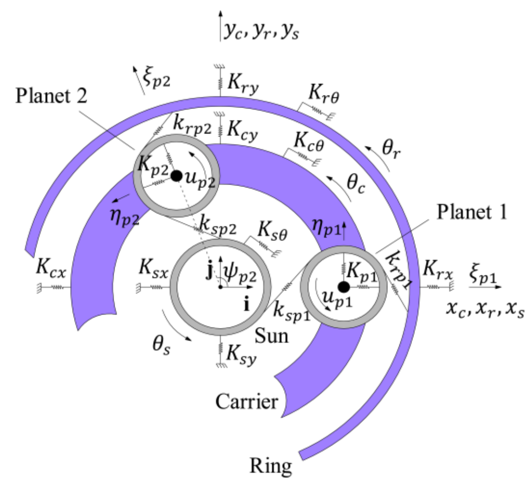

Fig. 1 Lumped parameter model of the planetary gear and system coordinates.

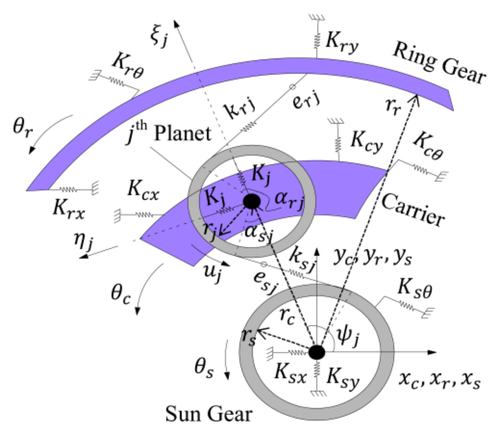

Fig. 2 Mesh of sun, ring and jth planet bearings.

Figure 3 shows the kinematics sketches to derive relative deflection of components. As an example for mesh of sun gear and jth planet gear, the gear mesh deflection (δ_{sj}) is obtained from the mixture of sun and jth planet deflections along the action line (“Fig. 3(a)”). Similarly, for mesh of ring gear and jth planet the gear mesh deformation (δ_{rj}) is derived by kinematics analysis of “Fig. 3(b)”. Kinematics analysis of “Fig. 3(c)” also shows the radial and tangential interfaces (δ_{jr} and δ_{jt}) of the planet bearing with respect to the carrier. Compression of the elastic elements (δ) is defined as “Eqs. (1)–(4)”:

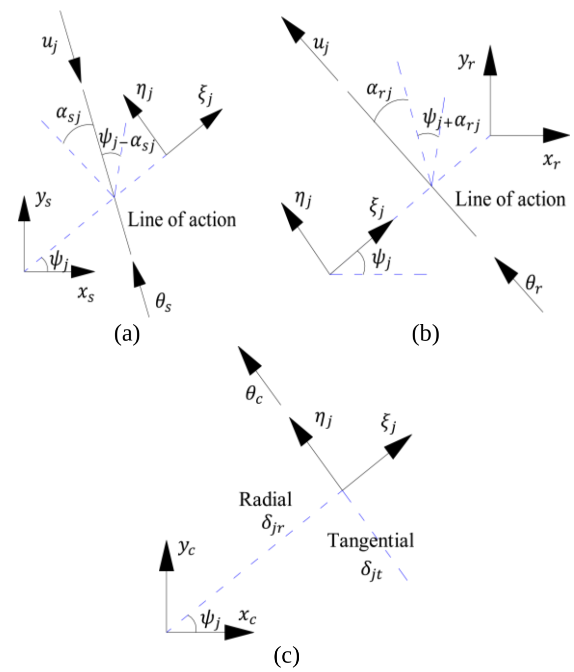

Fig. 3 Kinematics sketches to derive relative deflection components.

2.1 Mesh OF Sun– jth Planet

$$\delta_{sj} = \cos(\psi_j-\alpha_{sj})y_s - \sin(\psi_j-\alpha_{sj})x_s - \sin\alpha_{sj}\xi_j - \cos\alpha_{sj}\eta_j + r_s\theta_s + u_j + e_{sj}(t) \tag{1}$$

2.2 Mesh OF Ring– jth Planet

$$\delta_{rj} = \cos(\psi_j+\alpha_{rj})y_r - \sin(\psi_j+\alpha_{rj})x_r + \sin\alpha_{rj}\xi_j - \cos\alpha_{rj}\eta_j + r_r\theta_r - u_j + e_{rj}(t) \tag{2}$$

2.3 jth Planet Bearing Radial:

$$\delta_{jr} = \sin\psi_j y_c + \cos\psi_j x_c - \xi_j \tag{3}$$

2.4 jth Planet Bearing Tangential:

$$\delta_{jt} = \cos\psi_j y_c - \sin\psi_j x_c - \eta_j + r_c\theta_c \tag{4}$$

2.5 Equations OF Motion

According to degrees of freedom of the system, the system consists of $3(J+3)$ nonlinear equations of motion. Equations of motion for the single–stage spur planetary gear system of “Fig. 1” by the Newton’s second law are obtained as follows:

2.5.1 Carrier Equations

$$m_c\ddot{x}_c + K_j[(\sin\psi_j(t)y_c + \cos\psi_j(t)x_c - \xi_j)\cos\psi_j(t) - (\cos\psi_j(t)y_c - \sin\psi_j(t)x_c - \eta_j + r_c\theta_c)\sin\psi_j(t)] + K_{cy}y_c = 0 \tag{5}$$

$$m_c\ddot{y}_c + K_j[(\sin\psi_j(t)y_c + \cos\psi_j(t)x_c - \xi_j)\sin\psi_j(t) + (\cos\psi_j(t)y_c - \sin\psi_j(t)x_c - \eta_j + r_c\theta_c)\cos\psi_j(t)] + K_{cy}y_c = 0 \tag{6}$$

$$I_c\ddot{\theta}_c + K_j(\cos\psi_j(t)y_c - \sin\psi_j(t)x_c - \eta_j + r_c\theta_c) + K_{c\theta}\theta_c = 0 \tag{7}$$

2.5.2 Sun Gear Equations

$$m_s\ddot{x}_s - k_{sj}(t)(\cos(\psi_j(t)-\alpha_{sj}(t))y_s - \sin(\psi_j(t)- -\alpha_{sj}(t))x_s - \sin\alpha_{sj}(t)\xi_j - \cos\alpha_{sj}(t)\eta_j + r_s\theta_s + u_j + e_{sj}(t))\sin(\psi_j(t)-\alpha_{sj}) + K_{sx}x_s = F_{sx}(t) \tag{8}$$

$$m_s\ddot{y}_s + k_{sj}(t)(\cos(\psi_j(t)-\alpha_{sj}(t))y_s - \sin(\psi_j(t)- \alpha_{sj}(t))x_s - \sin\alpha_{sj}(t)\xi_j - \cos\alpha_{sj}(t)\eta_j + r_s\theta_s + u_j + e_{sj}(t))\cos(\psi_j(t)-\alpha_{sj}(t)) + K_{sy}y_s = F_{sy}(t) \tag{9}$$

$$I_s\ddot{\theta}_s + k_{sj}(t)(\cos(\psi_j(t)-\alpha_{sj}(t))y_s - \sin(\psi_j(t)- \alpha_{sj}(t))x_s - \sin\alpha_{sj}(t)\xi_j - \cos\alpha_{sj}(t)\eta_j + r_s\theta_s + u_j + e_{sj}(t)) + K_{s\theta}\theta_s = \tau_s(t) \tag{10}$$

2.5.3 Ring Gear Equations

$$m_r\ddot{x}_r - k_{rj}(t)(\cos(\psi_j(t)+\alpha_{rj}(t))y_r - \sin(\psi_j(t)+ \alpha_{rj}(t))x_r + \sin\alpha_{rj}(t)\xi_j - \cos\alpha_{rj}(t)\eta_j + r_r\theta_r - u_j + e_{rj}(t))\sin(\psi_j(t)+\alpha_{rj}(t)) + K_{rx}x_r = 0 \tag{11}$$

$$m_r\ddot{y}_r + k_{rj}(t)(\cos(\psi_j(t)+\alpha_{rj}(t))y_r - \sin(\psi_j(t)+ \alpha_{rj}(t))x_r + \sin\alpha_{rj}(t)\xi_j - \cos\alpha_{rj}(t)\eta_j + r_r\theta_r - u_j + e_{rj}(t))\cos(\psi_j(t)+\alpha_{rj}(t))] + K_{ry}y_r = 0 \tag{12}$$

$$I_r\ddot{\theta}_r + k_{rj}(t)(\cos(\psi_j(t)+\alpha_{rj}(t))y_r - \sin(\psi_j(t)+ \alpha_{rj}(t))x_r + \sin\alpha_{rj}(t)\xi_j - \cos\alpha_{rj}(t)\eta_j + r_r\theta_r - u_j + e_{rj}(t)) + K_{r\theta}\theta_r = 0 \tag{13}$$

2.5.4 j^th Planet Equations

$$m_j\ddot{\xi}_j - k_{sj}(t)(\cos(\psi_j(t)-\alpha_{sj}(t))y_s - \sin(\psi_j(t)- \alpha_{sj}(t))x_s - \sin\alpha_{sj}(t)\xi_j - \cos\alpha_{sj}(t)\eta_j + r_s\theta_s + u_j + e_{sj}(t))\sin\alpha_{sj}(t) + k_{rj}(t)(\cos(\psi_j(t)+\alpha_{rj}(t))y_r - \sin(\psi_j(t)+\alpha_{rj}(t))x_r + \sin\alpha_{rj}(t)\xi_j - \cos\alpha_{rj}(t)\eta_j + r_r\theta_r - u_j + e_{rj}(t))\sin\alpha_{rj}(t) - K_{pn}(\sin\psi_j(t)y_c + \cos\psi_j(t)x_c - \xi_j + r_c\theta_c) = 0 \quad (14)$$

$$m_j\ddot{\eta}_j - k_{sj}(t)(\cos(\psi_j(t)-\alpha_{sj}(t))y_s - \sin(\psi_j(t)- \alpha_{sj}(t))x_s - \sin\alpha_{sj}(t)\xi_j - \cos\alpha_{sj}(t)\eta_j + r_s\theta_s + u_j + e_{sj}(t))\cos\alpha_{sj}(t) - k_{rj}(t)(\cos(\psi_j(t)+\alpha_{rj}(t))y_r - \sin(\psi_j(t)+\alpha_{rj}(t))x_r + \sin\alpha_{rj}(t)\xi_j - \cos\alpha_{rj}(t)\eta_j + r_r\theta_r - u_j + e_{rj}(t))\cos\alpha_{rj}(t) - K_j(\cos\psi_j(t)y_c - \sin\psi_j(t)x_c - \eta_j + r_c\theta_c) = 0 \quad (15)$$

$$\frac{I_j}{r_j^2}\ddot{u}_j + k_{sj}(\cos(\psi_j(t)-\alpha_{sj}(t))y_s - \sin(\psi_j(t)- \alpha_{sj}(t))x_s - \sin\alpha_{sj}(t)\xi_j - \cos\alpha_{sj}(t)\eta_j + +r_s\theta_s + u_j + e_{sj}(t)) - k_{rj}(t)(\cos(\psi_j(t)+\alpha_{rj}(t))y_r - \sin(\psi_j(t)+ \alpha_{rj}(t))x_r + \sin\alpha_{rj}(t)\xi_j - \cos\alpha_{rj}(t)\eta_j + r_r\theta_r - u_j + e_{rj}(t)) = 0 \quad (16)$$

3 NATURAL FREQUENCIES AND VIBRATION MODES

Equations of motion for the single–stage spur planetary gear system in the matrix form are written as follow:

$$\mathbf{M}\ddot{\mathbf{q}}(t) + \left[\mathbf{K_m}(t) + \mathbf{K_b}\right]\mathbf{q}(t) = \boldsymbol{\tau}(t) + \mathbf{F}(t) \quad (17)$$

Where, M is the inertia matrix, K_b is the diagonal support (bearing) stiffness matrix and $K_m(t)$ is the symmetric stiffness matrix. $\boldsymbol{\tau}(t)$ denotes the external torque and the external torque is exerted on the sun gear and $F(t)$ shows the static transmission error excitation. Vector of the general coordinate for the single–stage spur planetary system is:

$$\mathbf{q} = [x_c, y_c, \theta_c, x_r, y_r, \theta_r, x_s, y_s, \theta_s, \xi_{p1}, \eta_{p1}, u_{p1}, ..., \xi_J, \eta_J, u_J]^{\mathrm{T}} \quad (18)$$

Where, ω_i are natural frequencies and φ_i are vector of vibration modes which are obtained from the numerical method of [25]. In planetary gear systems, vibration modes are classified into three types of translational, rotational and planet modes [25].

4 CALCULATION OF THE MESH STIFFNESS

In “Fig. 2”, $k_{rj}(t)$ and $k_{sj}(t)$ are the periodically time–varying mesh stiffness of ring– j^th planet and also sun– j^th planet. The basic frequency of the system is ω_T and equals to: $\omega_T = \gamma_s Q_S Q_r/(Q_s + Q_r)$, where γ_s is the angular velocity of the sun and Q denotes the teeth number for the internal and external gears. The periodically time–varying mesh stiffness of ring– j^th planet and also sun– j^th planet in the form of Fourier series is obtained from “Eqs. (19) and (20)”. In “Eqs. (19) and (20)”, h_r and h_s are harmonic terms used to explain and show the periodic functions of $k_{rj}(t)$ and $k_{sj}(t)$. $k_{rp}(t)$ and $k_{sp}(t)$ are harmonic coefficients and are resulted from the Fourier series with the average amounts of k_{rp}^1 and k_{sp}^1.

$$k_{rj}(t) = k^1{}_{rp} + \sum_{j=1}^{h_r}[(k_{rp}^{2j}\cos(\omega_T t - 2\hat{\Delta}_{rj}\pi) + k_{rp}^{2j+1}\sin(\omega_T t - 2\hat{\Delta}_{rj}\pi)] \quad (19)$$

$$k_{sj}(t) = k^1{}_{sp} + \sum_{j=1}^{h_s}[(k_{sp}^{2j}\cos(\omega_T t - 2\Delta_{sj}\pi) + k_{sp}^{2j+1}\sin(\omega_T t - 2\Delta_{sj}\pi)] \quad (20)$$

In the present model, the phasing (phase angle) of sun– j^th planet is Δ_{sj}. The phasing of ring– j^th planet is $\hat{\Delta}_{rj}$ and equals to $\Delta_{sj} + \Delta_{sr}$ and Δ_{sr} is the phasing of sun and ring gear (the phase angle between mesh of ring– j^th planet and mesh of sun– j^th planet).

Generally, the mesh stiffness of gears at the mesh frequency is the function of different factors such as tooth parameters (pressure angle of gears), geometric parameters (diameter of gears) and material properties and varies with the gears rotation. For pairs of teeth in spur gears, the mesh stiffness is depended on factors and parameters of the gear such as module, number of teeth, pressure angle, face width, hub bore radius and material properties [17, 24]. The single mesh stiffness of a pair of teeth can be calculated by some stiffness of each tooth such as stiffness of bending (k_b), shear (k_s), axial (k_a), fillet–foundation (k_f,) and contact (k_h) according to “Eqs. (21)–(25)” [17, 24]:

$$\frac{1}{k_b} = \int_0^d \frac{(x\cos a_1 - h\sin a_1)^2}{EI_x} d_x \quad (21)$$

$$\frac{1}{k_s} = \int_0^d \frac{1.2\cos^2 a_1}{GA_x} d_x \quad (22)$$

$$\frac{1}{k_a}=\int_0^d \frac{\sin^2 a_1}{EA_x} d_x \tag{23}$$

$$\frac{1}{k_f}=\frac{\cos^2 a_1}{WE}(L*(u_f/s_f)^2+M*(u_f/s_f)+ P*(1+Q*\tan^2 a_1)) \tag{24}$$

$$\frac{1}{k_h}=\frac{4(1-\upsilon^2)}{\pi EW} \tag{25}$$

Where, W is the gear face width, E, G and ν are the Young's modulus, shear modulus and Poisson's ratio of the gear. Other parameters of "Eqs. (21)–(25)" are displayed in "Fig. 4" and defined in [17, 24]. The single and double tooth pair duration of the gear and the pinion are derived as the rotation of the pinion [22]. So, the overall effectual mesh stiffness for the single tooth pair meshing duration is obtained as:

$$k(\theta_p)=\frac{1}{\frac{1}{k_{bg}}+\frac{1}{k_{sg}}+\frac{1}{k_{ag}}+\frac{1}{k_{fg}}+\frac{1}{k_h}+\frac{1}{k_{bp}}+\frac{1}{k_{sp}}+\frac{1}{k_{ap}}+\frac{1}{k_{fp}}} \tag{26}$$

Where, $k(\theta)$ denotes the overall effectual mesh stiffness which is expressed as the function of pinion rotation. Subscripts g and p represent the gear and the pinion.

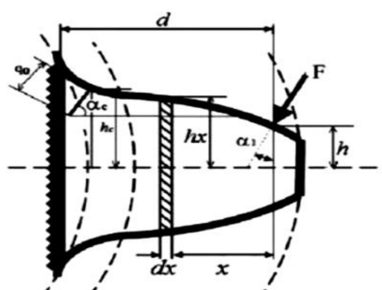

Fig. 4 Tooth parameters [24].

There are two pairs of gears meshing at the same time for the double tooth pair meshing duration. The overall effectual mesh stiffness for the double tooth pair meshing duration can be derived as:

$$k(\theta_p)=k_1(\theta_p)+k_2(\theta_p)= \sum_{i=1}^{2}\frac{1}{\frac{1}{k_{bg,i}}+\frac{1}{k_{sg,i}}+\frac{1}{k_{ag,i}}+\frac{1}{k_{fg,i}}+\frac{1}{k_{h,i}}+\frac{1}{k_{bp,i}}+\frac{1}{k_{sp,i}}+\frac{1}{k_{ap,i}}+\frac{1}{k_{fp,i}}} \tag{27}$$

Where $i = 1$ for the first pair of meshing teeth and $i = 2$ for the second pair of one. For the planetary gear the overall effectual mesh stiffness of sun–first planet and ring–first planet can be derived as the function of first planet rotation. So:

$$k_{s1}(t)=k(r_1\theta_1), k_{r1}(t)=k(r_1\theta_1) \tag{28}$$

Note that, because of mesh phasing relationships [7], the mesh stiffness of sun– j^th planet ($j = 2,3, \dots$) is the function of mesh stiffness of sun–first planet and relative phase between sun– j^th planet ($j = 2,3, \dots$) and sun–first planet. This is similar for the mesh stiffness of ring– j^th planet ($j = 2,3, \dots$). In this study, all sun– j^th planet and ring– j^th planet meshes have the same phase.

5 NUMERICAL RESULTS

Mesh stiffness of a tooth pair in some contact points (Fourier series coefficients), is obtained separately for both external (sun– j^th planet) and internal (ring– j^th planet) gears by design software of gear (MSC Marc software which investigates contact of gears by finite element method) for some pressure angles ("Fig. 5"). Fourier series coefficients of mesh stiffness function are resulted from the design software of gear. On the other hand, the profile of mesh stiffness function by the polynomial estimation function is resulted from the design software of gear.

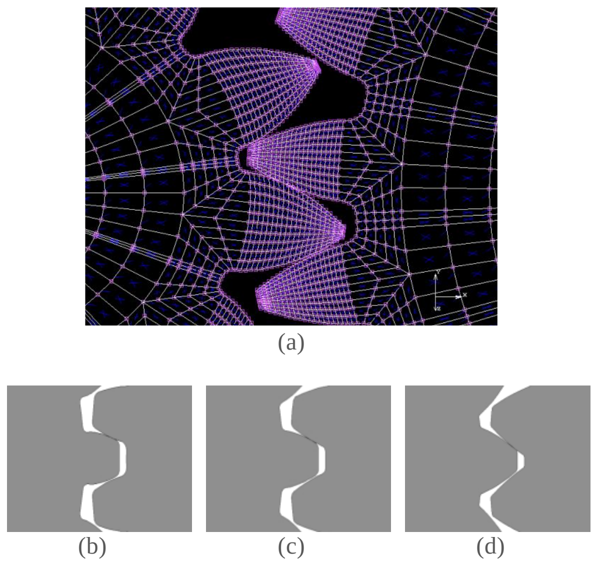

Fig. 5 Model of gear meshes by: (a) finite element with (b) 20° (c) 25° and (d) 30° pressure angle of gears.

Therefore, the periodically time–varying mesh stiffness of ring– j^th planet and also sun– j^th planet is produced by change in the number of contact tooth pairs for the rotational system in form of Fourier series of "Eqs. (19) and (20)" by the polynomial estimation function and system parameters of [25]. Moreover, 1.63 mm for the contact ratios, 20 mm for the teeth width, 206000 $\frac{N}{mm^2}$ for the Young's modulus, 1100 $N.m$ for the torque, 0.3 for the Poisson's ratio and 7850 $\frac{Kg}{m^3}$ for the density are considered for gears parameters. All sun– j^th planet and ring– jth planet meshes have same phase ($\Delta_{sj}= \hat{\Delta}_{rj}$). It means that all sun– jth planet and ring– jth planet mesh stiffnesses have same profile. Time–varying mesh stiffness of meshing gears is shown in “Figs. 6 and 7” along the action line.

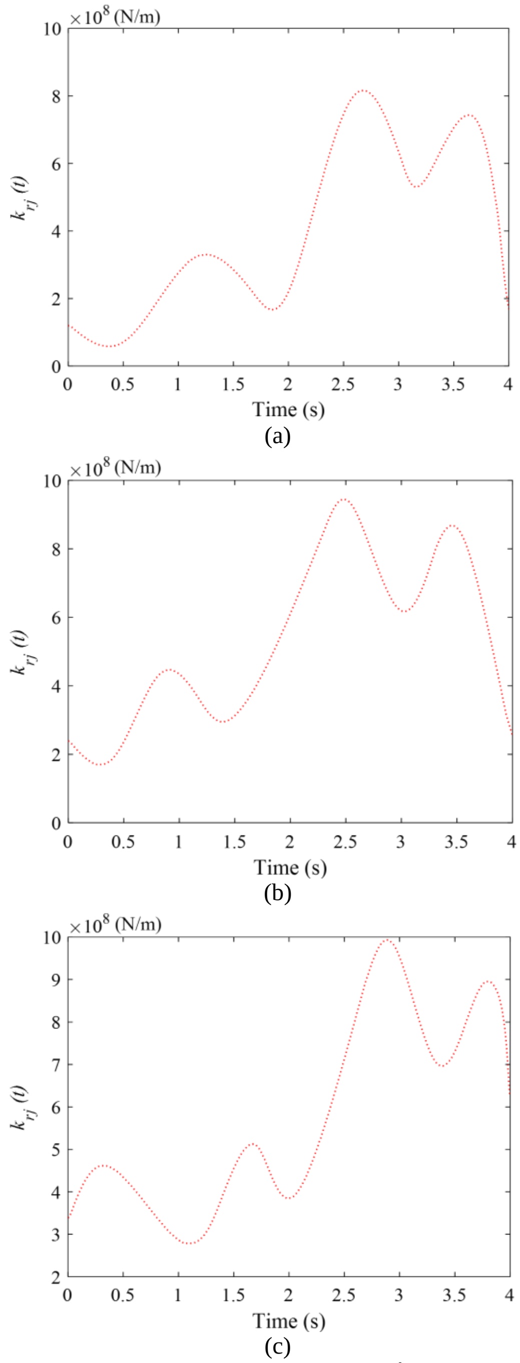

Fig. 6 Mesh stiffness variations of ring– jth planet with: (a) $\alpha_{rj} = 20^{\circ}$, (b) $\alpha_{rj} = 25^{\circ}$ and (c) $\alpha_{rj} = 30^{\circ}$.

In “Figs. 6 and 7”, the influence of pressure angles on the mesh stiffness of gears is shown. The influence of the higher pressure angles on the mesh stiffness of gears is perceptible. Similarly, it can be concluded that the influence of the other parameters such as gears diameter and the number of teeth on the mesh stiffness of gears is observable.

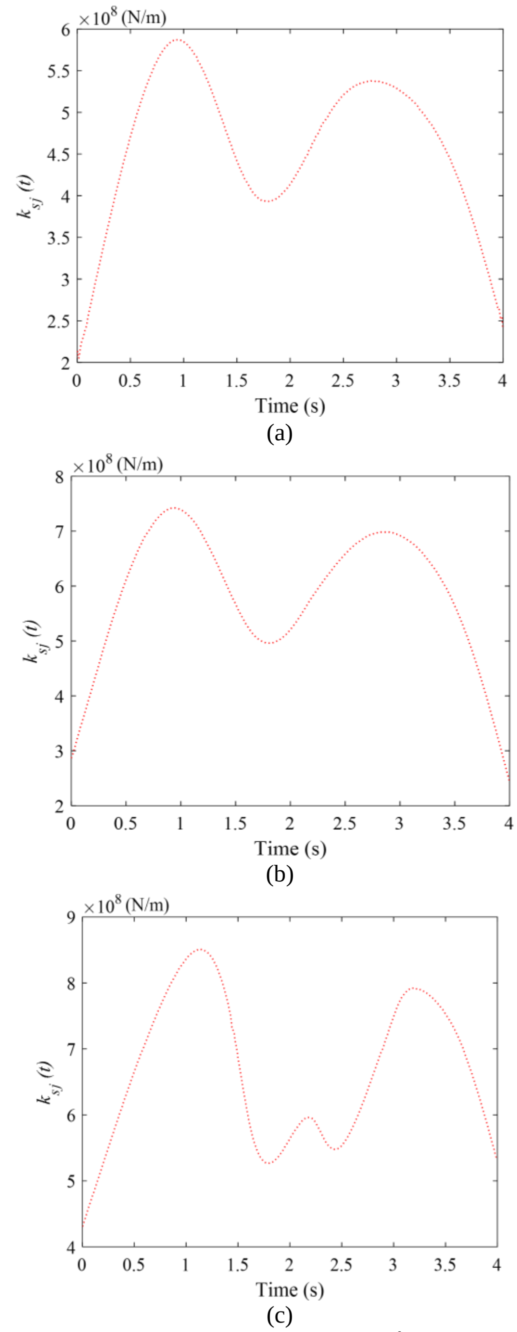

Fig. 7 Mesh stiffness variations of sun– jth planet with: (a) $\alpha_{sj} = 20^{\circ}$, (b) $\alpha_{sj} = 25^{\circ}$ and (c) $\alpha_{sj} = 30^{\circ}$.

For a pair of meshing gears, the overall effectual mesh stiffness can be converted to the overall effectual mesh stiffness of sun–first planet and ring–first planet in the planetary gear system. The mesh stiffness of sun–first planet and ring–first planet is obtained from "Eq. (28)" as the function of first planet rotation ("Figs. 8 and 9"). In this study, all sun– jth planet and ring– jth planet meshes are in the phase with each other in the planetary gear system ($\Delta_{sj} = \hat{\Delta}_{rj}$).
All sun– jth planet and ring– jth planet mesh stiffness have the same profile. The time–varying mesh stiffness of sun–first planet and ring–first planet is produced by change in the number of contact tooth pairs. The time–varying mesh stiffness of gears by parameters of [25] is obtained as "Figs. 8 and 9".

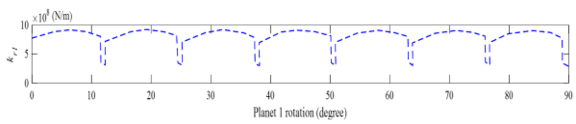

Fig. 8 Mesh stiffness variations of ring–first planet.

Table 1 Natural frequencies and vibration modes of ASS and SS with three planets

	ASS with $J=3$	SS with $J=3$	SS with $J=3$ [25]	Vibration mode
Natural frequencies [HZ] with multiplicity one	0	0	0	Rotational
	1476.9	1476.1	1475.7	Rotational
	1932.2	1931.9	1930.3	Rotational
	2661.7	2660.6	2658.3	Rotational
	7469.5	7466.1	7462.8	Rotational
	11780.1	11782.3	11775.2	Rotational
Natural frequencies [HZ] with multiplicity two	—	744.1	743.2	Translational
	—	1103.2	1102.4	Translational
	—	898.51	1896.0	Translational
	—	2278.9	2276.4	Translational
	—	6999.8	6986.3	Translational
	—	9652.4	9647.9	Translational
Natural frequencies [HZ] with multiplicity $J-3$	—	—		planet

"Table 1" and "Table 2" also show for the system with numbers of even unequally spaced planets (ASS with $J=4$), natural frequencies of translational modes have multiplicity one. When numbers of planets of the system are odd and the position of them is unequally spaced (ASS with $J=3$) natural frequencies of translational modes are omitted (have multiplicity zero) and other unknown modes are appeared on the system.

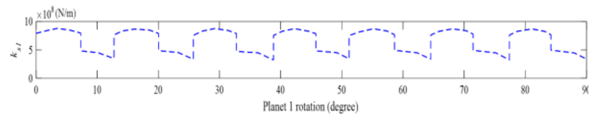

Fig. 9 Mesh stiffness variations of sun–first planet.

Table 2 Natural frequencies and vibration modes of ASS and SS with four planets

	ASS with $J=4$	SS with $J=4$	SS with $J=4$ [25]	Vibration mode
Natural frequencies [HZ] with multiplicity one	0	0	0	Rotational
	1537.3	1537.1	1536.6	Rotational
	1972.5	1971.6	1970.6	Rotational
	2627.9	2627.4	2625.7	Rotational
	7778.4	7789.8	7773.6	Rotational
	13080.7	13082.5	13071.1	Rotational
Natural frequencies [HZ] with multiplicity two	—	728.1	727	Translational
	—	1092.3	1091	Translational
	—	1893.9	1892.8	Translational
	—	2344.5	2342.5	Translational
	—	7194.2	7189.9	Translational
	—	10445.6	10437.6	Translational
Natural frequencies [HZ] with multiplicity $J-3$	1809.2	1809.9	1808.2	Planet
	5967.4	5967	5963.8	Planet
	6987.2	6987.9	6981.7	Planet
Natural frequencies [HZ] with multiplicity one	714.3, 739.9	—	—	Translational
	1086.5, 1097.9	—	—	Translational
	1860.2, 1938.8	—	—	Translational
	2333.6, 2359.1	—	—	Translational
	7054.6, 7330.8	—	—	Translational
	9903.5, 10960.1	—	—	Translational

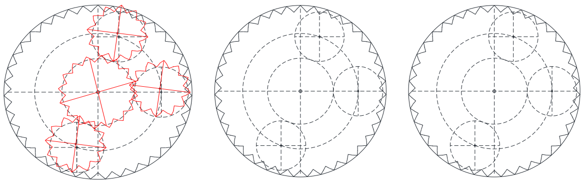

(a) Rotational mode: ω_6 =1476.9 Hz
(b) Planet mode: $\omega = -$
(c) Translational mode: $\omega = -$

Fig. 10 Types of vibration modes of the ASS with three planets (0, 80 and 260 degrees).

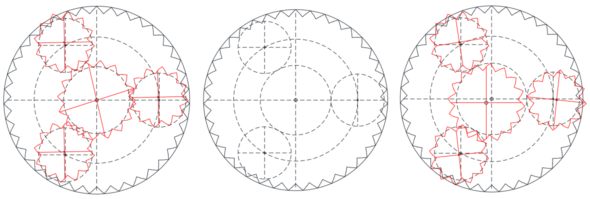

(a) Rotational mode: ω_6 =1476.1 Hz
(b) Planet mode: $\omega = -$
(c) Translational mode: ω_2 = 744.1 Hz

Fig. 11 Types of vibration modes of the SS with three planets (0, 120 and 240 degrees).

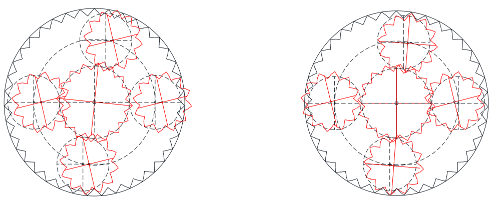

(a) Rotational mode: ω_6 = 1537.3 Hz
(b) Planet mode: ω_7 = 1809.2 Hz

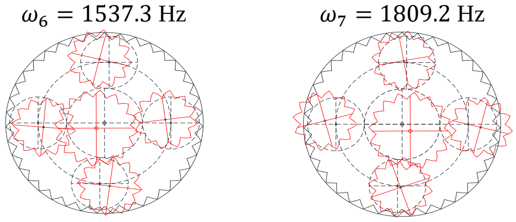

(c) Translational mode: ω_8 = 1860.2 Hz
(d) Translational mode: ω_8 = 1938.8 Hz

Fig. 12 Types of vibration modes of the ASS with four planets (0, 80, 180 and 260 degrees).

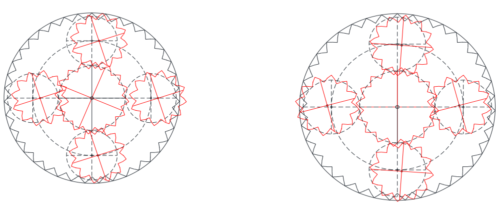

(a) Rotational mode: ω_6 = 1537.1 Hz
(b) Planet mode: ω_7 = 1809.9 Hz

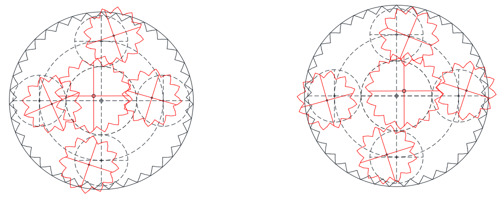

(c) Translational mode: ω_2 = 728.1 Hz
(d) Translational mode: ω_2 = 728.1 Hz

Fig. 13 Types of vibration modes of the SS with four planets (0, 90, 180 and 270 degrees).

6 CONCLUSION

In this paper, the dynamic of single–stage spur planetary gear is investigated. The planetary gear set is modeled as a set of lumped masses and springs. Each element such as sun gear, carrier, ring gear and planets possesses three degrees of freedom and is considered as rigid body. The periodically time–varying mesh stiffness of ring– jth planet and also sun– jth planet in form of Fourier series and finite element method is obtained by the polynomial estimation function. With calculating the overall effectual mesh stiffness for the single tooth pair meshing, the mesh stiffness of gears in the planetary gear system is investigated as the function of first planet rotation. The influence of gear parameters on the mesh stiffness of gears is obtained. For the system with numbers of odd and even equally and unequally spaced planets, natural frequencies and vibration modes are investigated. According to results, the inherent factors such as tooth parameters, geometric parameters and material properties are affected on the periodically time–varying mesh stiffness of gears. As an example, the influence of the higher pressure angles on the mesh stiffness of meshing gears is perceptible. Similarly, this result can be expanded for other parameters such as gears diameter and teeth number of gears. The mesh stiffness of sun–all planets has the same profile and also it can occurr for ring–all planets if all sun– jth planet and ring– jth planet are in the phase with each other. Furthermore, by using the proposed mesh stiffness of meshing gears, for the system with numbers of odd and even equally and unequally spaced planets, natural frequencies and vibration modes are obtained and validated with a high accuracy.

REFERENCES

[1] Li, S., Wu, Q., and Zhang, Z., Bifurcation and Chaos Analysis of Multistage Planetary Gear Train, Nonlinear Dynamics, Vol. 75, No. 1-2, 2014, pp. 217-233.

[2] Chen, E., and Walton, D., The Optimum Design of KHV Planetary Gears With Small Tooth Differences, International Journal of Machine Tools and Manufacture, Vol. 30, No. 1, 1990, pp. 99-109.

[3] Lin, J., and Parker, R., Planetary Gear Parametric Instability Caused by Mesh Stiffness Variation, Journal of Sound and vibration, Vol. 249, No. 1, 2002, pp. 129-145.

[4] Sun, T., and Hu, H., Nonlinear Dynamics of a Planetary Gear System with Multiple Clearances, Mechanism and Machine Theory, Vol. 38, No. 12, 2003, pp. 1371-1390.

[5] Saxena, A., Parey, A., and Chouksey, M., Effect of Shaft Misalignment and Friction Force on Time Varying Mesh Stiffness of Spur Gear Pair, Engineering Failure Analysis, Vol. 49, 2015, pp. 79-91.

[6] Hao, Z., Xianghe, Y., Qingkai, H., and Hai, H., Dynamic Behaviors of Geared Rotor System in Integrally Centrifugal Compressor, Journal of Vibration Engineering & Technologies, Vol. 7, 2019, pp. 241-249.

[7] Parker, R. G., and Lin, J., Mesh Phasing Relationships in Planetary and Epicyclic Gears, Journal of Mechanical Design, Vol. 126, No. 2, 2004, pp. 365-370.

[8] Inalpolat, M., and Kahraman, A., A Dynamic Model to Predict Modulation Sidebands of a Planetary Gear Set Having Manufacturing Errors, Journal of Sound and Vibration, Vol. 329, 2010, pp. 371-393.

[9] Wei, S., Han, Q. K., Dong, X. J., Peng, Z. K., and Chu, F. L., Dynamic Response of a Single-Mesh Gear System with Periodic Mesh Stiffness and Backlash Nonlinearity Under Uncertainty, Nonlinear Dynamics, Vol. 89, No. 1, 2017, pp. 49-60.

[10] Ambarisha, V. K., and Parker, R. G., Nonlinear Dynamics of Planetary Gears Using Analytical and Finite element Models, Journal of Sound and Vibration, Vol. 302, No. 3, 2007, pp. 577-595.

[11] Li, C. H., Chiou, H. S., Hung, C., Chang, Y. Y., and Yen, C. C., Integration of Finite Element Analysis and Optimum Design on Gear Systems, Finite Elements in Analysis and Design, Vol. 38, No. 3, 2002, pp. 179-192.

[12] Chen, Z. G., Shao, Y. M., and Lim, T. C., Non-Linear Dynamic Simulation of Gear Response Under the Idling Condition, International Journal of Automotive Technology, Vol. 13, No. 4, 2012, pp. 541-552.

[13] Kahraman, A., Natural Modes of Planetary Gear Trains, Journal of Sound Vibration, Vol. 173, 1994, pp. 125-130.

[14] Kahraman, A., Load Sharing Characteristics of Planetary Transmissions, Mechanism and Machine Theory, Vol. 29, No. 8, 1994, pp. 1151-1165.

[15] Liu, L., Niu, J., and Li, X., Dynamic Analysis of Gear System Under Rractional-Order PID Control with the Feedback of Meshing Error Change Rate, Acta Mechanica, Vol. 229, 2018, pp. 3833-3851

[16] Masoumi, A., Pellicano, F., Samani, F. S., and Barbieri, M., Symmetry Breaking and Chaos-Induced Imbalance in Planetary Gears, Nonlinear Dynamics, Vol. 80, 2015, pp. 561-582.

[17] Sainsot, P., Velex, P., and Duverger, O., Contribution of Gear Body to Tooth Deflections-a New Bidimensional Analytical Formula, Journal of Mechanical Design, Vol. 126, No. 4, 2004, pp. 748-752.

[18] Shen, Y., Yang, S., and Liu, X., Nonlinear Dynamics of a Spur Gear Pair with Time-Varying Stiffness and Backlash Based on Incremental Harmonic Balance Method, International Journal of Mechanical Sciences, Vol. 48, No. 11, 2006, pp. 1256-1263.

[19] Shi, J. F., Gou, X. F., and Zhu, L. Y., Modeling and Analysis of a Spur Gear Pair Considering Multi-State Mesh with Time-Varying Parameters and Backlash, Mechanism and Machine Theory, Vol. 134, 2019, pp. 582-603.

[20] Wang, J., and Howard, I., The Torsional Stiffness of Involute Spur Gears, Proceedings of the Institution of Mechanical Engineers, Part C: Journal of Mechanical Engineering Science, Vol. 218, No. 1, 2004, pp. 131-142.

[21] Zhou, X., Shao, Y., Lei, Y., and Zuo, M., Time-Varying Meshing Stiffness Calculation and Vibration Analysis for a 16DOF Dynamic Model with Linear Crack Growth in a Pinion, Journal of Vibration and Acoustics, Vol. 134, No. 1, 2012.

[22] Tian, X., Zuo, M. J., and Fyfe, K. R., Analysis of the Vibration Response of a Gearbox with Gear Tooth Faults. In ASME 2004 International Mechanical Engineering Congress and Exposition, American Society of Mechanical Engineers Digital Collection, 2004, pp. 785-793.

[23] Jin, G., Ren, W., Zhu, R., and Lu, F., Influence of Backlash on Load Sharing and Dynamic Load Characteristics of Twice Split Torque Transmission System, Journal of Vibration Engineering & Technologies, Vol. 7, 1999, pp. 565-577.

[24] Yang, D., and Sun, S., A Rotary Model for Spur Gear Dynamics, Journal of Mechanical Design, Vol. 107, No. 4, 1985, pp. 529-535.

[25] Lin, J., and Parker, R. G., Analytical Characterization of the Unique Properties of Planetary Gear Free Vibration, Journal of Vibration and Acoustics, Vol. 121, 1999, pp. 316-321.